IOP Conf. Series: Materials Science and Engineering **263** (2017) 022015 doi:10.1088/1757-899X/263/2/022015

Optical field induced rotation of polarization in rubidium atoms with the additional magnetic field

M Ummal Momeen and Jianping Hu
School of Advanced Sciences, VIT University, Vellore Campus, Vellore- 632014, Tamil Nadu, India

E-mail : ummalmomeen@gmail.com, jianpinghu@hotmail.com

Abstract. We present the magnetic and optical field induced rotation of polarization in ^{87}Rb and ^{85}Rb atoms at geophysical magnetic fields. The line shape varies considerably in the presence of a magnetic field of the order of a few mG. Multiple Zeeman sublevel EIT systems involving rubidium atoms are investigated. Theoretical formalism of optical field induced polarization rotation in the presence of a magnetic field is discussed by considering all the Zeeman sublevels. It is noted that the ground state population distribution also plays a major role.

1. Introduction

In recent years there has been significant interest in the study of atoms/molecules in electromagnetic fields. Strong polarization rotation in magneto-optical effects are used in sensitive magnetometry for time reversal-invariance violation experiments and search for electron dipole moment measurements[1]. It is fascinating that extremely slow propagation of light, lasing without inversion and quantum information devices rely on the basic mechanisms of electromagnetically induced transparency (EIT) and coherent population trapping (CPT) [2]. Under the appropriate conditions, coherent superposition of two ground states coupled through a common upper state lead to EIT/CPT. Optically/magnetically controlled polarization rotation has important applications in switching devices, locking mechanism and quantum information processing [3-4]. EIT in an alkali atomic vapor is rich in literature; there are several others who have discussed this mechanism in various forms [5-10]. The existence of magneto- chiral effect is important in atom- laser interaction measurements [11]. Agarwal and Dasgupta [12] shown that it is possible to produce very large magneto chiral effect using electromagnetically induced coherence in a resonant atomic medium. Electromagnetically induced chirality is applicable to atoms, molecules, quantum dots, excitons, etc. Electromagnetically induced transparency (EIT) in a magnetic chiral medium was discussed by Sautenkov et al., [13]. Xiao et al., [14] have studied the EIT in an atomic medium for Rb atomic vapors. Controlling the polarization rotation of an optical field via asymmetry in EIT has been discussed by Wang et al. Self rotation in Rb atomic vapor has been identified in elliptically polarized incident light. It is extensively discussed that self rotation is due to optical pumping effects, ac- Stark shifts and Stark quantum beats [15].

In this work, we have used the basic concepts of chirality and self rotation so that the polarization rotation angle can be controlled by a strong circularly-polarized optical field as well as by an applied static magnetic field. Optical fields induce polarization rotation in an atomic medium via optical pumping. The pumping process produces an unequal population distribution among the ground

state Zeeman sublevels. Such an anisotropic system become birefringent and dichroic for an incident linearly polarized probe beam. Its plane of rotation is rotated after having passed the anisotropic sample. In order to enhance the Faraday rotation, both magnetic and optical fields are used to control the anisotropy in an atomic medium. In the presence of a magnetic field the Zeeman sublevels of different F levels are non-degenerate. The ground/excited state splits into different Zeeman sublevels on the application of magnetic field. The frequency shifts among various Zeeman sublevels lead to magneto-optical rotation. Wang et al., [16] studied the optical field induced polarization rotation for the D_1 line in the absence of magnetic field. This work emphasizes the signature of EIT and Faraday rotation at geophysical magnetic fields.

The line shape is analyzed as a function of probe laser detuning for different magnetic fields. The optical field breaks the symmetry in a number of EIT subsystems and the symmetry breaking manifests as a difference in dispersion of the left and right- circularly-polarized components of the linearly polarized weak probe beam. This has been studied for the ^{87}Rb and ^{85}Rb D_2 lines by realizing multi-configuration Λ systems. We have also shown how EIT in the presence of magnetic field can be used successfully to produce a large asymmetry in these systems. We have also analyzed the effect of Doppler broadening and ac- Stark shifts in this configuration.

2. Theoretical Formalism

A circularly polarized, strong control beam induces birefringence effects while a linearly polarized, weak probe beam detects the anisotropy in an atomic medium. The control laser beam is much stronger than the probe laser beam. Under weak probe conditions, it can be demonstrated that only two-photon processes are important in this approximation; therefore complicated multilevel systems are reduced to a simple three-level Λ type EIT system. The linearly polarized probe beam is a combination of left (σ_-) and right (σ_+) circularly polarized components. The multiple Zeeman sublevel system can be considered as a superposition of different three-level systems. In the case of ^{87}Rb, we have considered the control laser beam transition as F=2 to F'=2 and the probe beam transition as F=1 to F'=2. There are three different three-level Λ type EIT subsystems for the (σ_+, σ_+) control and probe polarization configuration. Similarly there are two different three-level Λ type EIT subsystems and a single two-level system in the (σ_+, σ_-) control and probe polarization configuration. This leads to a circular asymmetry, which induces birefringence in an atomic medium. The corresponding Zeeman sublevels of F=1, F=2 and F'=2 in ^{87}Rb are labeled as $|a_i\rangle$, $|b_j\rangle$ and $|c_k\rangle$ where i=1, 2, 3; j=1, 2, 3, 4, 5 and k=1, 2, 3, 4, 5. In the case of ^{85}Rb, F=3 to F'=3 is regarded as control laser beam transition and F=2 to F'=3 as probe beam transition. Hence there are five different three-level Λ type EIT subsystems for the (σ_+, σ_+) control and probe polarization configuration. Similarly there are four different three-level Λ type EIT subsystems and a single two-level system in the (σ_+, σ_-) control and probe polarization configuration. For the sake of brevity, only the ^{87}Rb level system and the corresponding equations are discussed below.

A schematic diagram of multi-Zeeman sublevel ^{87}Rb is shown in figure 1.

Faraday rotation; $\varphi = \frac{\pi l}{2\lambda} Re(\chi^+ - \chi^-)$ (1)

where l is the length of the sample; χ^+ is the atomic susceptibility for the right circularly polarized probe component, χ^- is the atomic susceptibility for the left circularly polarized probe component and λ is the wavelength of light. The accurate description of the characteristics of polarization rotation signals is obtained from an analysis of density matrix equations for the atomic polarizations. All coupled Zeeman sublevels are taken into account in the analysis of the magnetic and optical field induced birefringence effects.

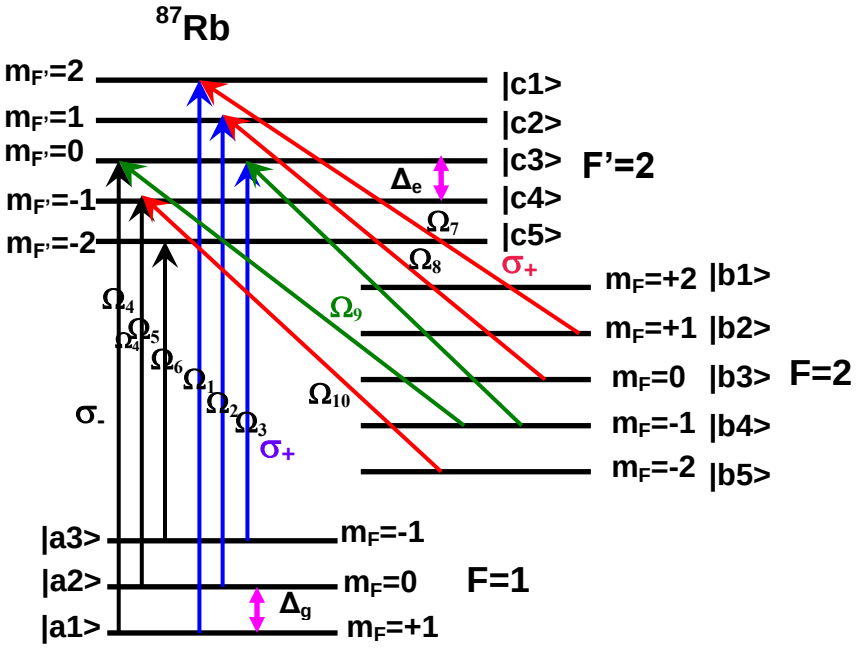

Figure 1. ^{87}Rb energy level scheme for multi-level Λ configuration

In the case of ^{87}Rb, the susceptibilities for the right circularly and left circularly polarized probe components can be written as

$$\chi^{+} = \frac{-2N}{\hbar\varepsilon_0}\left[\frac{|\mu_{a1c1}|^2}{\Omega_1}\rho_{c1a1} + \frac{|\mu_{a2c2}|^2}{\Omega_2}\rho_{c2a2} + \frac{|\mu_{a3c3}|^2}{\Omega_3}\rho_{c3a3}\right]$$

$$\chi^{-} = \frac{-2N}{\hbar\varepsilon_0}\left[\frac{|\mu_{a1c3}|^2}{\Omega_4}\rho_{c3a1} + \frac{|\mu_{a2c4}|^2}{\Omega_5}\rho_{c4a2} + \frac{|\mu_{a3c5}|^2}{\Omega_6}\rho_{c5a3}\right] \quad (2)$$

Ω_1, Ω_2, Ω_3- Rabi frequencies for the right circularly polarized component of probe atomic transitions and Ω_4, Ω_5, Ω_6- Rabi frequencies for the left circularly polarized component of probe atomic transitions. Ω_7, Ω_8, Ω_9, Ω_{10} are for the control (pump) atomic transitions. ρ is the density matrix term, μ is the dipole moment for the appropriate atomic transition.

The Rabi frequency is given by: $\Omega = \frac{-\mu.E}{\hbar}$, where E is the electric field. The probe Rabi frequencies are much weaker than the control laser Rabi frequencies. Hence it is considered that the higher order terms of probe Rabi frequencies are negligible in the calculation.

In steady state, it is assumed that $\sum \rho_{aa} = 1$ and $\sum \rho_{bb} = \sum \rho_{cc} = 0$. When the strong control laser beam couples to the levels $|b\rangle$ to $|c\rangle$, it can also interact with the corresponding Zeeman sublevels in the neighboring F levels. For ^{87}Rb, there are two possible ways in which this interaction can happen, i.e. F=2 to F'=1 ($m_{F'}$= -1, $m_{F'}$= 0, $m_{F'}$= +1) levels and F=2 to F'=3 ($m_{F'}$= -1, $m_{F'}$= 0, $m_{F'}$= +1, $m_{F'}$= +2) levels. Such interactions induce ac-Stark shifts. They are denoted as δ_1, δ_2, δ_3 for the F=2 to F'=1 level and as δ_a, δ_b, δ_c, δ_d for the F=2 to F'=3 levels. Here $\delta_i = \frac{|\Omega_i|^2}{4\Delta}$, where Δ is the energy difference between the two appropriate hyperfine excited levels. In the realistic comparison of experimental results with the calculated values, Doppler effect due to atomic motion needs to be taken into account by integrating over the atomic velocity distribution. If an atom moves against the propagation direction of the probe and coupling beams with velocity u, the one-photon frequency detuning will

change as: $\Delta_p = \Delta_p + kv;\ \Delta_c = \Delta_c + kv$; where $k = \frac{2\pi}{\lambda}$, λ is the wavelength of light. The coupling and probe beams are co-propagating in the atomic cell and this eliminates the first-order Doppler broadening in two-photon frequency detuning $(\Delta_1 - \Delta_2)$. Under the weak probe field approximation the density matrix terms for ^{87}Rb are written as:

$$\tilde{\rho}_{c1a1} = \int_{-\infty}^{+\infty} \frac{\frac{i\Omega_1}{2}\tilde{\rho}_{a1a1}}{\left[i(\Delta_1 + kv + 2\Delta_e - \Delta_g) - \Gamma_{c1a1}\right] + \frac{\frac{\Omega_7^2}{4}}{[i[(\Delta_1 - \Delta_g) - (\Delta_2 + \Delta_g) + \delta_a] - \Gamma_{b2a1}]}} N(u)du.$$

$$\tilde{\rho}_{c2a2} = \int_{-\infty}^{+\infty} \frac{\frac{i\Omega_2}{2}\tilde{\rho}_{a2a2}}{\left[i(\Delta_1 + kv + \Delta_e) - \Gamma_{c2a2}\right] + \frac{\frac{\Omega_8^2}{4}}{[i[(\Delta_1 - \Delta_2) + \delta_1 + \delta_b] - \Gamma_{b3a2}]}} N(u)du.$$

$$\tilde{\rho}_{c3a3} = \int_{-\infty}^{+\infty} \frac{\frac{i\Omega_3}{2}\tilde{\rho}_{a3a3}}{\left[i(\Delta_1 + kv + \Delta_g) - \Gamma_{c3a3}\right] + \frac{\frac{\Omega_9^2}{4}}{[i[(\Delta_1 + \Delta_g) - (\Delta_2 - \Delta_g) + \delta_2 + \delta_c] - \Gamma_{b4a3}]}} N(u)du.$$

$$\tilde{\rho}_{c3a1} = \int_{-\infty}^{+\infty} \frac{\frac{i\Omega_4}{2}\tilde{\rho}_{a1a1}}{\left[i(\Delta_1 + kv - \Delta_g) - \Gamma_{c3a1}\right] + \frac{\frac{\Omega_9^2}{4}}{[i[(\Delta_1 - \Delta_2) + \delta_2 + \delta_c] - \Gamma_{b4a1}]}} N(u)du.$$

$$\tilde{\rho}_{c4a2} = \int_{-\infty}^{+\infty} \frac{\frac{i\Omega_5}{2}\tilde{\rho}_{a2a2}}{\left[i(\Delta_1 + kv - \Delta_e) - \Gamma_{c4a2}\right] + \frac{\frac{\Omega_{10}^2}{4}}{[i[\Delta_1 - (\Delta_2 - 2\Delta_g) + \delta_3 + \delta_d] - \Gamma_{b5a2}]}} N(u)du.$$

$$\tilde{\rho}_{c5a3} = \int_{-\infty}^{+\infty} \frac{\frac{i\Omega_6}{2}\tilde{\rho}_{a3a3}}{[i(\Delta_1 + kv - 2\Delta_e + \Delta_g) - \Gamma_{c5a3}]} N(u)du. \quad (3)$$

N(u) is the velocity distribution which obeys the Maxwellian distribution .

$$N(u)du = N\frac{1}{v\sqrt{\pi}}\exp\left(-u^2/v^2\right)du \quad (4)$$

where 'v' is the root-mean-square atomic velocity. Here Γ 's are decay terms and Ω is the Rabi frequency. Rabi frequencies are calculated for different atomic transitions by using the appropriate transition strength of a given atomic transition. Zeeman shifts in the atomic ground and excited states are termed as Δ_g and Δ_e respectively.

Zeeman shift = $\frac{g_F \mu_B m_F B}{\hbar}$. (5)

3. Results and Discussion

The calculated results for ^{87}Rb is shown in figure 2. There is an additional window which appears with the increase in magnetic field. It is found at a magnetic field of 500 mG in ^{87}Rb. There is no significant change in the rotation at smaller fields (<500 mG). It is perhaps because these smaller magnetic fields (a few MHz) are weak in comparison with other effects such as detuning frequency (hundreds of MHz) and Stark shifts (a few MHz). The magnetic field is of the order of a few MHz and it is within the linewidth of the atomic transitions. Hence the theoretical calculations are limited by the complexity of solving all the coupled differential equations in the density matrix formalism.

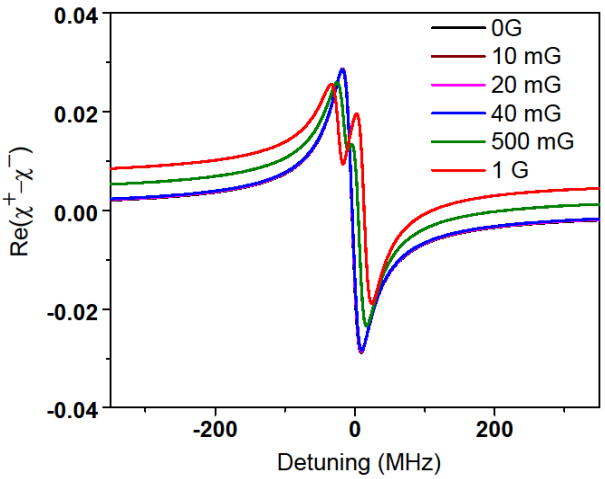

Figure 2. Optical/magnetic field induced polarization rotation for ^{87}Rb.

The calculations are made by assuming the ground state population, $\rho_{a1a1} = \rho_{a2a2} = \rho_{a3a3} = 0.33$ and the decay terms $\Gamma_{ba} = 2\pi \times 1$ MHz; $\Gamma_{ca} = \Gamma_{cb} = 2\pi \times 3.5$ MHz; Here the Zeeman shift for ^{87}Rb D2 line ground state is 4.39 MHz/G and for the excited state (F'=2) 5.84 MHz/G. The Stark shifts are $\delta_1 = 2.32$ MHz; $\delta_2 = 2.32$ MHz; $\delta_3 = 1.55$ MHz ; $\delta_a = 0.91$ MHz; $\delta_b = 1.36$ MHz; $\delta_c = 1.36$ MHz; $\delta_d = 0.91$ MHz;

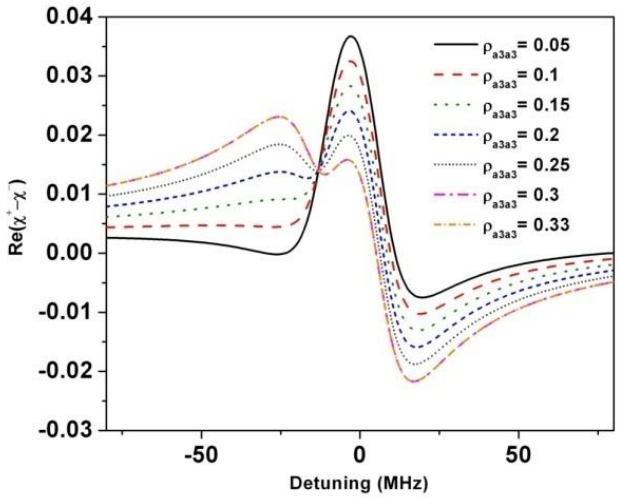

Figure 3. ^{87}Rb Optical/magnetic field induced rotation as a function of ground state population (ρ_{a3a3}).

Magnetic-field-dependent terms and also ac-Stark shifts of the susceptibility decomposition terms are showing nonlinear behaviour in the presence of electromagnetic fields. These non linear factors are responsible for the enhancement of polarization rotation. Figure 3 shows how rotation varies with the ground state population distribution for B=500 mG. The line shape changes drastically with the population. Due to optical pumping and Stark shifts, it is expected that ground state cannot be equally populated at higher laser power. The Zeeman shift of ^{85}Rb D2 line atomic ground state is 2.93 MHz/G and for the excited state (F'=3) 3.42 MHz/G.

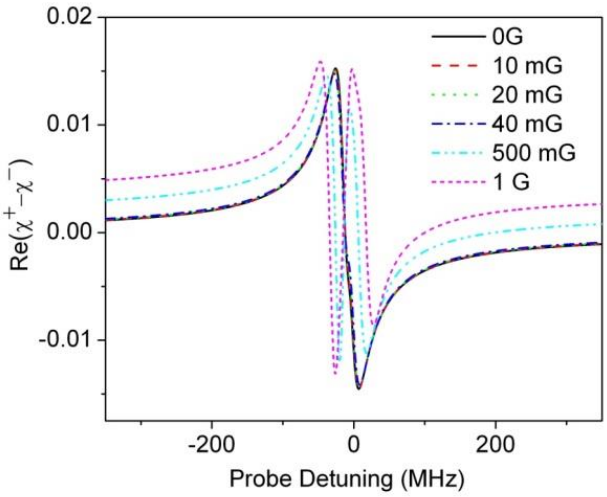

Figure 4. Optical/magnetic field induced polarization rotation for ^{85}Rb.

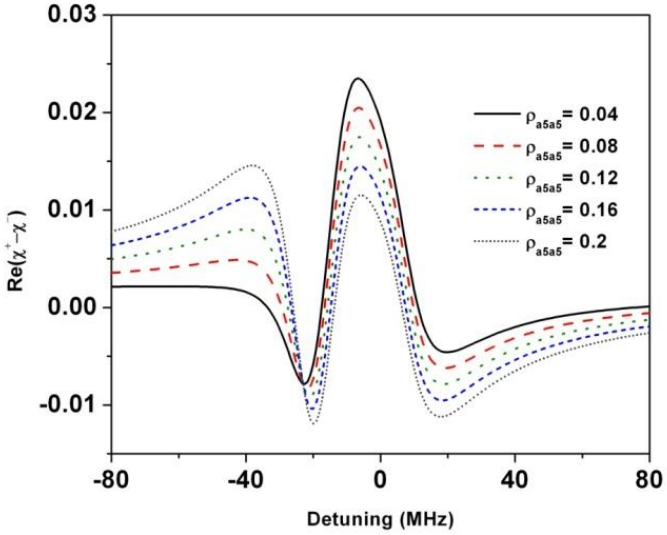

Figure 5. ^{85}Rb Optical/magnetic field induced rotation as a function of ground state population.

In the calculation the ground state population are assumed as $\rho_{a1a1} = \rho_{a2a2} = \rho_{a3a3} = \rho_{a4a4} = \rho_{a5a5} = 0.2$; Stark shift values are $\delta_1 = 5.35$ MHz; $\delta_2 = 6.4$ MHz; $\delta_3 = 6.4$ MHz; $\delta_4 = 5.35$ MHz; $\delta_5 = 3.2$ MHz; $\delta_a = 1.67$ MHz; $\delta_b = 2.78$ MHz; $\delta_c = 3.34$ MHz; $\delta_d = 3.34$ MHz; $\delta_e = 2.78$ MHz; $\delta_f = 1.67$ MHz; The calculated results are shown in figure 4. Figure 5 shows the influence of population distribution in rotation at B=500 mG. It clearly indicates that the ground state population distribution play a role in this magnetic field induced optical rotation. These theoretical simulations can be adopted to design a high sensitive magnetometer based on rubidium atomic vapor cell.

4. Summary and conclusions

Large asymmetry has been observed for the magnetic field of the order of a few mG. The enhancement of polarization rotation is due to self rotation (influence of Stark shifts) and also different combination of polarization configuration for the control and probe laser beams which induces the

asymmetry in the multi level rubidium atomic system. Ground state atomic distribution also plays a major role in these studies. Rotation changes its sign with the increase in magnetic field of the order of a few mG, this concept can be manipulated to construct a high sensitive magneto-optic switching device with atomic systems. From these studies we can conclude that the application of additional optical and magnetic fields results in the improvement in magneto-optical rotation. These enhancement in magneto-optical rotation can be utilized for designing atomic vapor cell magnetometers.

References

[1] Budker D, Gawlik W, Kimball D F, Rochester S M, Yashchuk V V and A Weis 2002 *Rev. Mod. Phys.* **74** 1153
[2] Novikova I, Phillips D F and Walsworth R L 2007 *Phys. Rev. Lett.* **99** 173604
[3] Eisaman M D, André A, Massou F, Fleischhauer M, Zibrov A S and Lukin M D 2005 *Nature* **438** 837
[4] Bell S C, Heywood D M, White J D, Close J D and Scholten R E 2007 *Appl. Phys. Lett.* **90** 171120
[5] Renzoni F, Lindner A and Arimondo E 1999 *Phys. Rev. A* **60** 450
[6] Sautenkov A, Lukin M D, Bednar C J, Novikova I, Mikhailov E, Fleischhauer M, V. L. Velichansky V L, Welch G R and Scully M O 2000 *Phys. Rev. A* **62** 023810
[7] Phillips D F, Fleischhauer M, Mair A, Walsworth R L and Lukin M D 2001 *Phys. Rev. Lett.* **86** 783
[8] Javan A, Kocharovskaya O, Lee H and Scully M O 2002 *Phys. Rev. A* **66** 013805
[9] Fleischhauer M, Imamoglu A and Marangos J P 2005 *Rev. Mod. Phys.* **77** 633
[10] Tan B, Tian Y, Lin H, Chen J and Gu S 2015 *Opt. Lett.* **40** 3703
[11] Vallet M, Ghosh R, Le Floch A, Ruchon T, Bretenaker F and Thépot J -Y. 2001 *Phys. Rev. Lett.* **87** 183003
[12] Agarwal G S and Dasgupta S 2003 *Phys. Rev. A* **67**, 023814
[13] Sautenkov V A, Rostovtsev Y V, Chen H, Hsu P, Agarwal G S and Scully M O 2005 *Phys. Rev. Lett.* **94** 233601
[14] Xiao M, Li Y Q, Jin S Z and Banacloche J G 1995 *Phys. Rev. Lett.* **74** 666
[15] Rochester S M, Hsiung D S, Budker D, Chiao R Y, Kimball D F and Yashchuk V V 2001 *Phys. Rev. A* **63** 043814
[16] Wang B, Li S, Ma J, Wang H, Peng K C and Xiao M 2006 *Phys. Rev. A* **73** 051801(R)